BIOLOGY OF REPRODUCTION (2013) **89**(2):48, 1–13
Published online before print 19 June 2013.
DOI 10.1095/biolreprod.112.107185

The Role of Fibroblast Growth Factor Receptor Substrate 2 (FRS2) in the Regulation of Two Activity Levels of the Components of the Extracellular Signal-Regulated Kinase (ERK) Pathway in the Mouse Epididymis[1]

Bingfang Xu, Ling Yang, and Barry T. Hinton[2]

Department of Cell Biology, University of Virginia Health System, Charlottesville, Virginia

ABSTRACT

The components of the extracellular signal-regulated kinase (ERK) pathway are involved in the regulation of epididymal cellular processes. Interestingly, our previous studies showed that there are two different activity levels of the ERK pathway components in the epididymal epithelium: a basal level in most regions and a higher level in the differentiated initial segment (IS). In this study we analyzed the role of fibroblast growth factor receptor substrate 2 (FRS2) in the regulation of these two levels. Two mouse models were generated. In the first model, *Frs2* was deleted from epithelial cells of most epididymal regions except for the IS from the embryonic period onward. Loss of *Frs2* dampened the basal activity level of the ERK pathway components, which resulted in an increase in apoptosis along the epididymal duct. This was observed during the period when FRS2 expression level was highest in wild-type epididymides. In the second model, *Frs2* was deleted from the proximal epididymal epithelium from Postnatal Day 17 onward. Most of the epididymides in this model exhibited normal morphology. Loss of *Frs2* in these epididymides did not affect the high activity level of the ERK pathway components in the IS. However, a subgroup of epididymides in the second model showed increased apoptosis which resulted in an abnormally shaped proximal region or development of granulomas. Therefore, data from these two models showed that FRS2 played different roles in the regulation of two activity levels of the ERK pathway components in the epididymis.

apoptosis, epididymal development, ERK pathway, FRS2, transgenic/knockout model

INTRODUCTION

The mammalian epididymis consists of a single coiled duct which is approximately 6 m long in humans and 1 m in the mouse [1, 2]. This long, convoluted epididymal duct provides a luminal fluid microenvironment for sperm maturation, transportation, and storage. It is not surprising that without a fully developed and functional epididymis, male infertility will result [3].

The epididymis develops from the anterior part of Wolffian duct. During embryonic development, the epididymal duct undergoes dramatic tubular elongation and convolution [1, 4]. Postnatal epididymal development can be divided into three periods: 1) the undifferentiated period in which the low columnar cell layers of epididymal epithelium are essentially undifferentiated [5]; 2) the period of differentiation in which the columnar epithelial cells differentiate into the principal, narrow/clear, halo, and basal cells [6] and four epididymal regions: the initial segment (IS), the caput, the corpus, and the cauda, begin to exhibit distinct morphology and function [6]; and 3) the period of expansion during which spermatozoa appear within the epididymal lumen and the organ length and weight increase significantly [2, 5]. In rodents these three postnatal periods span approximately Postnatal Day 1 (P1)–P15, P15–P44, and P44–adult, respectively [5].

In the course of epididymal development, the components of the extracellular signal-regulated kinase (ERK) pathway play many roles in the regulation of epididymal cellular processes. Interestingly, by analyzing the phosphorylation level of mitogen-activated protein kinases 3 and 1 (MAPK3/1) and the transcription levels of their down-stream target genes, including dual specificity phosphatase 6 (*Dusp6*), dual specificity phosphatase 5 (*Dusp5*), ets variant gene 4 (*Etv4*), and ets variant gene 5 (*Etv5*), we found two activity levels of the components of the ERK pathway in the epididymal epithelium: a basal level and a much higher level [7, 8].

The basal activity level of the components of the ERK pathway was found in epithelial cells in all epididymal regions prior to the period of differentiation and remained in most epithelial cells except for the IS epithelium from the period of differentiation onward. Targeted deletion of *Dusp6*, a negative regulator of the ERK pathway, resulted in an increase of this basal activity level, which led to an increase in cell proliferation in the caput and corpus [8]. Therefore, this basal activity level has been suggested to be important for cell proliferation in these regions.

The high activity level of components of the ERK pathway was established only in the IS epithelium from P17 onward [8], coincident with the first wave of testicular luminal fluid reaching the epididymis [9]. In addition, when we prevented luminal fluid from entering the IS by performing an efferent duct ligation (EDL), this high activity level of the ERK pathway components was abolished [7, 8], indicating that testicular luminal fluid contained factors (i.e., lumicrine factors) responsible for the activation of the components of the ERK pathway. Our previous study also demonstrated that abolishment of the high activity level of the ERK pathway components by EDL resulted in cessation of cell proliferation and differentiation in the IS epithelium of juvenile mice and resulted in a wave of apoptosis in the IS epithelium of adult mice [7, 8]. Therefore, the high activity level of the ERK pathway components was essential for cell proliferation, differentiation, and survival of the IS epithelium [7, 8].

[1]This work was supported by National Institutes of Health Eunice Kennedy Shriver National Institute of Child Health and Development grants HD052035 and HD068365.
[2]Correspondence: Barry T. Hinton, Department of Cell Biology, University of Virginia Health System, PO Box 800732, Charlottesville, VA 22908. E-mail: bth7c@virginia.edu

Received: 19 December 2012.
First decision: 25 January 2013.
Accepted: 6 June 2013.

eISSN: 1529-7268 http://www.biolreprod.org
ISSN: 0006-3363

Fibroblast growth factor receptor substrate 2 (FRS2, also known as FRS2alpha) is a major adapter protein for several receptor tyrosine kinases (RTKs). Activation of the RTKs by growth factor signaling allows FRS2 to become phosphorylated at tyrosine residues and then activates ERK, phosphatidyl inositol (PI)-3 kinase, and ubiquitination/degradation pathways. Therefore, FRS2 acts as a major regulator in multiple signal transduction pathways [10]. Ablation of *Frs2* from prostatic epithelial precursor cells disrupted the activation of MAPK3/1, impaired prostatic ductal branching morphogenesis, and compromised cell proliferation [11]**.** Ablation of *Frs2* in cardiac outflow tract progenitor cells compromised activation of the components of the ERK pathway, which resulted in outflow tract misalignment and hypoplasia [12]. Deletion of *Frs2* from ureteric epithelium affected the ret proto-oncogene (RET) signaling pathway components in kidney development and caused renal hypoplasia [13]. All these studies demonstrated that FRS2 regulates the development and function of multiple organs through ERK or other signal transduction pathways.

To study the role of FRS2 in epididymal development and its role in the regulation of two activity levels of the components of the ERK pathway, we generated two conditional knockout mouse models. In the first model, Hoxb7-Cre was used to conditionally knock out *Frs2*. The homeobox B7 (*Hoxb7*) gene encodes a transcription factor involved in cell proliferation and differentiation [14]. Expression of Hoxb7-Cre was detected as early as Embryonic Day 9.5 (E9.5) in the mesonephric duct and was then detected later in mesonephric derivatives (the Wolffian/epididymal duct, the collecting duct epithelium of kidney, and the ureteral epithelium) [14]. Therefore, in the first model, *Frs2* was deleted from most epididymal regions from the embryonic period onward to test the role of FRS2 in regulation of the basal activity level of ERK pathway components. In the second model, RNase10-Cre was used to conditionally knock out *Frs2*. *RNase10* was identified as the gene expressed particularly in the proximal epididymis [15]; a recent knock out study indicated it is involved in sperm maturation [16]. Expression of RNase10-Cre begins on approximately P17 with strong expression in the IS and proximal caput but wanes gradually distally without a distinct border [15]. Therefore, in the second model, *Frs2* was deleted from the proximal epididymis from P17 onward to test the role of FRS2 in regulation of the high activity level of ERK pathway components. Our findings based on these two models suggest that FRS2 regulates the basal activity level of ERK pathway components and is important for cell survival during the undifferentiated period of epididymal development. FRS2 does not regulate the high activity level of ERK pathway components and has no significant effect on cell survival from the period of differentiation onward.

MATERIALS AND METHODS

Animals

Mice were handled according to approved protocols, following the guidelines of the Institutional Animal Care and Use Committee (IACUC) of the University of Virginia. Mice carrying the *loxP*-flanked *Frs2* allele ($Frs2^{flox/flox}$) were a generous gift from Dr. Wang (University of Texas A&M) [11, 12, 17]. Trangenic (Tg) (RNase10-Cre) mice were a generous gift from Dr. Huhtaniemi (Imperial College London, UK) [15]. The Tg (Hoxb7-Cre) mouse line was generated in Dr. McMahon's laboratory (Harvard University) [14]. Tg (EIIa-Cre) mice (B6.FVB-Tg [EIIa-cre] C5379Lmgd/J) were purchased from Jackson Laboratory (Jax no. 003724; Jackson Laboratory, Bar Harbor, ME). The EIIa-Cre-mediated recombination occurs in a wide range of tissues including the germ cells that transmit the genetic alternation to progeny. This EIIa-Cre line was bred with $Frs2^{flox/flox}$ to generate $Frs2^{+/-}$ mice.

The mT/mG Cre reporter mice (Gt [ROSA] $26Sor^{tm4\ [ACTB-tdTomato,-EGFP]\ Luo}$/J; Jax no. 007676) and the luciferase Cre reporter mice (Gt [ROSA] $26Sor^{tm1\ [Luc]\ Kael}$/J; Jax no. 005125) were purchased from Jackson Laboratory. The mT/mG Cre reporter mice possess *loxP* sites on either side of the membrane-targeted tdTomato (mT) cassette and express strong red fluorescence in all tissues. When mT/mG Cre reporter mice are bred to Cre recombinase-expressing mice, the resulting offspring have the mT cassette deleted in the *cre*-expressing tissue(s), allowing expression of the membrane-targeted EGFP (mG) cassette. This double-fluorescent system allows direct visualization of both recombined and nonrecombined cells at single-cell resolution. The luciferase Cre reporter mice contain the firefly luciferase gene inserted into the *Gt* (*ROSA*)*26Sor* locus. Expression of the luciferase gene is blocked by a *loxP*-flanked STOP fragment placed between the luciferase gene and the *Gt* (*ROSA*)*26Sor* promoter. When mT/mG Cre reporter mice are bred to Cre recombinase-expressing mice, successful Cre-mediated excision is indicated by luciferase expression in Cre-expressing tissues. Mice were bred and genotyped as described in previous reports [11, 12, 14, 15, 17].

Western Blot Analysis

Tissue pieces from the IS and caput were homogenized in ice-cold radioimmunoprecipitation assay buffer with protease and phosphatase inhibitors (Thermo Fisher Scientific, Lake Barrington, IL). The homogenate was centrifuged (16 000 × *g* for 10 min) and analyzed using the Bradford protein assay (Bio-Rad, Hercules, CA). Proteins were separated by SDS-PAGE and then transferred to nitrocellulose membranes. Membranes were blocked in 5% fat-free dry milk with Tris-buffered saline (TBS), and incubated with the primary antibodies followed by 1:2000 dilution of alkaline phosphatase-conjugated secondary antibody (Sigma, St. Louis, MO) and then reacted with 1 Step NBT/BCIP (Thermo Fisher Scientific). The following primary antibodies were used for Western blot analysis: FRS2 antibody (1:200 working dilution; catalog no. sc-8318; Santa Cruz Biotechnology, Santa Cruz, CA), MAPK1 antibody (1:1000 working dilution; catalog no. 9108; Cell Signaling Technology, Beverly, MA), and MAPK3/1 antibody (1:1000 working dilution; catalog no. 4695; Cell Signaling Technology).

Immunofluorescence

Epididymal tissue samples were immersion fixed in 4% paraformaldehyde (PFA) in TBS overnight at 4°C, followed by paraffin embedding and sectioning of tissue samples. The knockout and control sections were placed side by side on the same slide to ensure similar treatment. Subsequently, slides were deparaffinized and rehydrated. For antigen retrieval, slides were microwaved in antigen-unmasking solution (Vector Laboratories, Burlingame, CA) for 10 min on high in a 1300-W microwave and cooled for 1 h at room temperature. After blocking in blocking solution with 10% (v/v) normal goat serum (Vector Laboratories), 0.5% (v/v) gelatin from cold-water fish skin (Sigma), and TBS for 1.5 h, slides were incubated overnight at 4°C in blocking solution with the primary antibodies, including the antibody against phospho-histone H3, a mitosis marker (1:500 working dilution; catalog no. 06–570; Millipore, Billerica, MA) or phospho-FRS2 (Y436) antibody (1:50 working dilution; catalog no. ab78195; Abcam, Cambridge, MA,), or phospho-FRS2 (Y196) antibody (Cell Signaling Technology, Beverly, MA, catalog # 3864, 1:50 working dilution). After being washed in TBS, slides were incubated with 1:200 dilution of Alexa Fluor 594 secondary antibody (Molecular Probes, Eugene, OR) in blocking solution for 1.5 h at room temperature. All slides were washed in TBS and mounted using Prolong anti-fade reagent with 4′,6-diamidino-2-phenylindole (DAPI) for nuclear staining (Molecular Probes) and viewed with a microscope equipped with epifluorescence (Zeiss).

Confocal Microscopy

Epididymal tissue samples from the mT/mG mice, which had been bred with the Cre lines, were fixed in 4% PFA overnight, were manually cut into 1-mm-thin pieces and mounted using Prolong anti-fade reagent (Molecular Probes) and then viewed with a confocal microscope (model LSM 510 ultraviolet; Zeiss).

Luciferase Assay

Assays were performed with a luciferase assay system (Promega, Fitchburg, WI) according to the manufacturer's instructions. Previously collected and frozen samples were ground with a mortar and pestle under liquid nitrogen. Proteins were extracted in cell culture lysis buffer. Protein determinations were made using the Bradford method (Bio-Rad). A single luciferase assay with 50 μg of protein in a 20-μl volume was performed using luciferase Assay Reagent

II (Promega). Measurements were made using a luminometer (model FB-15; Zylux Corp., Maryville, TN).

Immunohistochemistry

For immunohistochemistry (IHC), tissue slides were deparaffinized and then rehydrated. Endogenous peroxidases were quenched by incubation in 0.5% H_2O_2 in methanol for 30 min. After antigen retrieval, slides were blocked in the same blocking solution described above in the *Immunofluorescence* (IF) protocol for 1.5 h and were then blocked further in avidin D and biotin solution (Vector Laboratories) for 15 min respectively. Slides were then incubated overnight at 4°C with phospho-MAPK1/3 antibody (T202/Y204; working dilution 1:100; catalog no. 9101; Cell Signaling Technology) in blocking solution. After being washed in TBS, slides were incubated with a 1:200 dilution of biotinylated secondary goat anti-rabbit antibody (Vector Laboratories) in blocking solution for 1.5 h at room temperature. All slides were washed in TBS and incubated with avidin-biotin complex (Vectastain Elite ABC kit; Vector Laboratories) for 30 min at room temperature, reacted with diaminobenzidine (Sigma), and counterstained with Harris hematoxylin. Finally, slides were dehydrated, cleared with xylene, and mounted with permanent mounting medium (Vectamount; Vector Laboratories).

TUNEL Analysis

For TUNEL analysis, tissue samples were fixed, embedded, and sectioned as for IF. Rehydrated sections were irradiated by microwaving in a freshly prepared solution containing 0.1% Triton X-100 and 0.1% sodium citrate for 9 min. After being washed in PBS, slides were incubated in a TUNEL reaction mixture (Roche, Basel, Switzerland) for 1 h at 37°C in a humidified atmosphere in the dark. Reactions were stopped in PBS, and slides were mounted using Prolong anti-fade reagent (Molecular Probes) and viewed with a microscope equipped with epifluorescence (Zeiss). The epididymides from 10 pairs of the knockout ($Frs2^{cko/-}$ $Hoxb7\text{-}Cre^{tg}$) mice and their litter mate controls from the age of P4 to P10 were investigated. There were no changes in tubule diameter or cell density between the knockout epididymides and those of the litter mate controls; the apoptotic index was calculated as the number of apoptotic cells in the epithelium per square millimeter of epididymal area. A paired *t*-test was performed using Microsoft Excel software. Epididymal area was measured using Image J software (US National Institutes of Health; http://imagej.nih.gov/ij).

Real-Time PCR

Total RNA was isolated from P14 epididymides, excluding the IS, or from the IS and caput of adult (8-week-old) epididymides. Each group included four replicates. RNase-free DNase (Qiagen, Valencia, CA) was added to remove DNA contamination. First-strand cDNA was synthesized using Superscript synthesis system (Invitrogen, Carlsbad, CA). Real-time PCR quantification of mRNA levels was performed using SensiMix SYBR kit (Bioline, Tauton, MA). The *Frs2* primers *Frs2-F* (5′-ACCAAAAGAAGAGCCGAGTAACC-3′) and *Frs2-R* (5′-TTTCCCAGTTGCTCCAGTTTCTCC-3′) were designed to amplify the fragment of the last exon:. The primers for *Dusp6*, *Etv4*, *Etv5*, *Ret*, androgen receptor (*Ar*), c-ros oncogene 1 (*Ros1*), and wingless-related MMTV integration site 11 (*Wnt11*) were designed to span introns, as follows: *Dusp6-F* (5′-CGACTGGAATGAGAACACTGGTGG-3′) and *Dusp6-R* (5′-TCTA GATTGGTCTCGCAGTGCAGG-3′); *Etv4-F* (5′-GAAGGAGACATCAAG CAGGAAGG-3′) and *Etv4-R* (5′- CACCAGAAACTGCCACAGTTGTAAG-3′); *Etv5-F* (5′-GTCAAGCAGGAGCCCACCATGTATC-3′) and *Etv5-R* (5′-AGTGGGCATTGGCTGGGTCATC-3′); *Ret-F* (5′-CAATGAGAC TACTGGCCTTC-3′) and *Ret-R* (5′-AAAGACCTGGAGGAAGATGG-3′); *Ar-F* (5′-TGTGCCGGACATGACAACAACC-3′) and *Ar-R* (5′-TGCCATCTGGTCATCCACATGC-3′); *Ros1-F* (5′-CACTGATACAAGG CAATTCCGAG-3′) and *Ros1-R* (5′-TCCTTCACTCACCTTGCTTGACC -3′); and *Wnt11-F* (5′-AGGTCTGCGAGGCTCTGCTC-3′) and *Wnt11-R* (5′-CCAGGCCCTCCAGCTGTTTAC-3′). The amplified *18S* rRNA gene served as the loading control. Standard curves were generated with serial dilutions of a reverse transcription cDNA sample. A melting curve was adopted to analyze the specificity of PCR products. Data were analyzed using Excel software. The relative mRNA expression of target genes was normalized to the copy number of *18S* rRNA. In comparison experiments, the target gene:*18S* level ratio in the control was set as 1, and the relative values (means ± SEM) of the test experiment were then calculated. One-way ANOVA was performed to identify significant changes.

RESULTS

Dynamic Changes of FRS2 Expression and Localization During Epididymal Postnatal Development

FRS2 expression was investigated during the course of epididymal postnatal development by Western blot analysis (Fig. 1A). The most distinct changes were found between the ages of P14 and P21. As shown in Figure 1A, the FRS2 antibody, which reacted with all forms of FRS2, detected a series of protein bands of approximately 80 kDa. At the age of P14, both the undifferentiated IS and the caput showed high levels of FRS2 protein expression. From P21 onward, the expression level of FRS2 declined in both the IS and the caput, and the FRS2 bands shifted toward lower molecular weights in the caput (Fig. 1A).

FRS2 phosphorylation level and localization were studied by IF using a phospho-FRS2 antibody, which reacted with FRS2 phosphorylated at tyrosine 436 (Fig. 1B). A decrease in FRS2 phosphorylation level and a change of membrane-associated FRS2 localization were found between P14 and P21. In addition to weak cytoplasmic and nuclear labeling of phospho-FRS2 in the epithelial cells, strong phospho-FRS2 labeling was observed at both the basolateral and the apical membranes of epithelial cells, with no differences between each of the epididymal regions at P14 (Fig. 1, B1 and B2). From P21 onward, membrane-associated phospho-FRS2 was observed only at the apical region of the IS epithelium (Fig. 1, B3 and B5), and immunolabeling of phospho-FRS2 in the caput (Fig. 1, B4 and B6), corpus, and cauda was weak. Immunolabeling of phospho-FRS2 in mesenchymal cells and spermatozoa was visible but weak. Another phospho-FRS2 antibody, which reacted with FRS2 phosphorylated at Y196, was also used. A similar pattern was observed (data not shown), confirming these results.

Recombination Efficiency of the Hoxb7-Cre Line in the Epididymis

Because there is no published study, which used Hoxb7-Cre to conduct conditional targeted deletion in the epididymis, we investigated the recombination efficiency of the Hoxb7-Cre line in the epididymis by crossing those mice with the mT/mG Cre reporter line. The cells with green fluorescent labeling indicated successful recombination events (Fig. 2). A low-magnification image (Fig. 2A) of the proximal epididymal region of a P10 mT/mG mouse expressing Hoxb7-Cre showed negative recombination activity in the proximal IS, a low level of activity in the distal IS, and a stronger activity in the caput than in the IS. Confocal images showed that Hoxb7-Cre recombination activity was not detected in a proximal IS area at P10 (Fig. 2B). Hoxb7-Cre efficiently induced recombination events in more than 60% of epithelial cells in the caput (Fig. 2C), the corpus, and the cauda at P10. Therefore, the Hoxb7-Cre line was a useful tool for targeted gene deletion in epithelial cells of most epididymal regions except for the IS.

Phenotypes of Conditional Deletion of Frs2 Driven by Hoxb7-Cre

Epididymides with conditional deletion of *Frs2* driven by Hoxb7-Cre ($Frs2^{cko/-}$ $Hoxb7\text{-}Cre^{tg}$) were compared with those of their litter mate controls, with the genotype of either $Frs2^{flox/-}$ or $Frs2^{cko/+}$ $Hoxb7\text{-}Cre^{tg}$. FRS2 proteins were efficiently removed from most of the epididymal epithelium except for the IS epithelium in the P10 knockout mice (Fig. 3, A and B).

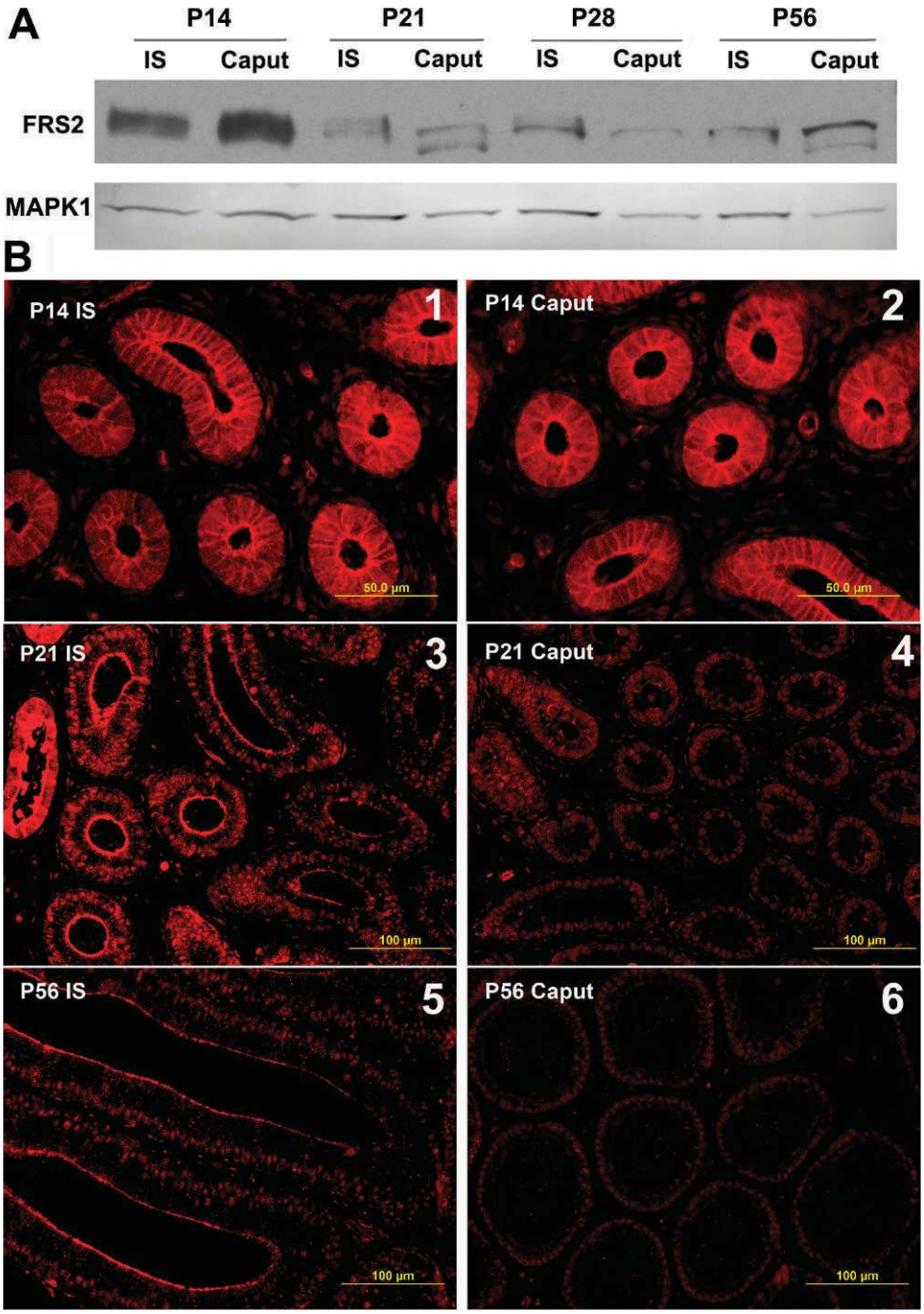

FIG 1. Expression and localization patterns of FRS2 in the IS and caput regions during postnatal development. **A**) Western blot analysis of FRS2 expression from P14 to P56 in the IS and caput regions. A series of strong bands of approximately 80 kDa were detected by a total FRS2 antibody from P14 IS and caput samples. From P21 onward, the expression level of total FRS2 declined, and the FRS2 bands shifted toward lower molecular weights in the caput, presumably because of dephosphorylation. **B**) Representative figures of phospho-FRS2 immunolocalization in the IS and caput from P14 to P56. Phospho-FRS2 was localized to both the basolateral and the apical membranes of epithelial cells at P14 with no differences between the IS and caput. Then, phospho-FRS2 was observed to be concentrated at the apical membrane of the IS epithelial cells from P21 onward. Weak cytoplasmic and nuclear labeling of phospho-FRS2 was also observed. Bar = 50 μm (**B1** and **B2**) or 100 μm (**B3–B6**).

Western blot analysis confirmed that FRS2 protein expression level in the P10 knockout epididymal tissues (excluding the IS) was reduced compared to that of controls (Fig. 3C). The epididymides of the knockout mice looked grossly normal during all postnatal epididymal development periods examined. Cell proliferative activity was not affected by deletion of *Frs2* (data not shown). However, an increase in apoptosis was detected during the undifferentiated period after loss of *Frs2*. As shown in Figure 3E, the epididymides from 10 pairs of knockout mice and their litter mate control mice were investigated. Apoptotic indexes in the control and knockout mice were 5.67 ± 1.45 and 12.42 ± 2.32 (means ± SEM), respectively (paired *t*-test; the *P* one-tail value from this test was less than 0.05). The clusters of apoptotic cells were found along the epididymal duct (Fig. 3D) in the knockout mice, but these clusters did not accumulate in the epithelium. Instead, the apoptotic cells were often observed inside the lumen (data not shown). Neither the

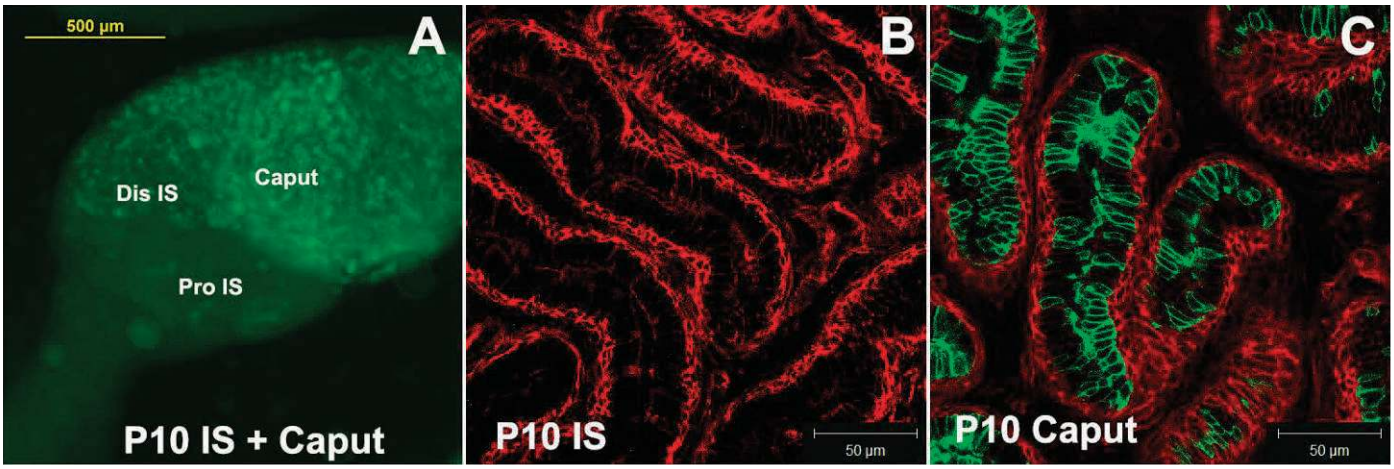

FIG 2. Recombination efficiency of Hoxb7-Cre at P10. Recombination efficiency of Hoxb7-Cre was tested by breeding Hoxb7-Cre mice with mT/mG Cre reporter mice. The change of fluorescent color on the cell membrane from red to green indicated a recombination event induced by Hoxb7-Cre. **A**) A low magnification image of the proximal epididymal region at P10 showing a negative recombination activity in the proximal IS (Pro-IS) and a low level of activity in the distal IS (Dis IS) and a higher level of activity in the caput. **B**) A confocal image showing that Hoxb7-Cre recombination activity was not detected in a proximal IS area at P10. **C**) A representative image showing that recombination occurred in more than 60% of epithelial cells in a caput region at P10. Bars = 500 μm (**A**) or 50 μm (**B** and **C**).

clustered apoptotic cells nor the increase in apoptosis was observed from the period of differentiation onward.

Impact of Frs2 *Deletion Driven by Hoxb7-Cre on the Components of Signal Transduction Pathways During the Undifferentiated Period*

Quantitative PCR was used to analyze changes in mRNA expression of several genes following *Frs2* ablation by Hoxb7-Cre during the undifferentiated period. First, we confirmed that following deletion of *Frs2* from epithelial cells, *Frs2* mRNA expression in P14 knockout epididymal tissues (excluding IS tissues) declined to ~36% of the control level, and this decline was shown to be significant ($P < 0.01$). Consistent with the lower *Frs2* expression, the mRNA expression of three ERK pathway downstream genes, *Etv4*, *Etv5*, and *Dusp6*, significantly decreased (Fig. 4, upper panel) in the knockout group. However, genes that belonged to other pathways, *Ret*, *Ros1*, *Ar*, and *Wnt11*, did not show significant changes in their mRNA expression levels (Fig. 4, lower panel) following loss of *Frs2*.

Recombination Efficiency of the RNase10-Cre Line

In our second mouse model, the Cre recombinase driven by the *RNase10* promoter was used to delete the target gene from epithelial cells of the proximal epididymis from P17 onward. To test the efficiency of this Cre line, RNase10-Cre mice were crossed with mT/mG Cre reporter mice. Recombination events induced by RNase10-Cre began at P17, and by P21, they had reached their maximal efficiency (data not shown). As shown in Fig. 5, in adult mice, recombination events occurred in most of the epithelial cells in the IS epithelium (Fig. 5, A2 and A1, lower tubule) but not in narrow cells (Fig. 5A, 2, arrows), whose apical cytoplasm often protrudes into the lumen [3]. A mosaic recombination pattern was found in the proximal caput epithelium (Fig. 5A, 3), where the recombination activity was gradually reduced from the proximal to the distal caput. Only a few leaky recombination events were detected in the corpus (Fig. 5A, 4) and efferent ducts (Fig. 5A, 1, upper tubule).

RNase10-Cre mice were also crossed with luciferase Cre reporter mice, and then luciferase activity was quantified to indicate recombination efficiency of RNase10-Cre (Fig. 5B). Compared to the low background in the RNase10-Cre nonexpressing littermate controls, RNase10-Cre drove a high level of recombination in the IS, and recombination efficiency was approximately 80% less in the caput compared to the IS.

Phenotypes of Frs2 *Conditional Deletion Driven by RNase10-Cre*

Conditional deletion of *Frs2* from epithelial cells of the proximal epididymis from P17 onward resulted in abnormal epididymal morphology in approximately 22% of the total number of adult epididymides (Table 1). The abnormality had a wide range of severity. In the most severe cases, the proximal epididymides were absent or much smaller in the knockout mouse than in the control (Fig. 6A). Abnormally shaped proximal epididymides were also observed (Fig. 6, B and C). Obstruction (Fig. 6D, arrow heads) and consequent development of granulomas (Fig. 6D, arrow) were detected in the proximal region of knockout epididymides. Although sporadic granulomas were seen in the control groups, the incidence of granulomas was higher in the knockout groups than in the control groups, based on examination of a large number of epididymides (each group including 22–118 epididymides) (Table 1). The sites of granuloma in the knockout groups were usually in the proximal epididymis, while it was observed in every region in the control groups.

Because approximately 77% of epididymides with the $Frs2^{cko/cko}$ *RNase10-Cre*^{tg} genotype appeared grossly normal (Table 1), two more mouse lines were generated to ensure efficient deletion of *Frs2*. In the first line, ($Frs2^{cko/cko}$ *RNase10*-Cre$^{tg/tg}$), two alleles of RNase10-Cre were present. In the second line, (Frs2$^{cko/-}$ RNase10-*Cre*^{tg}), one *Frs2* allele was already knocked out, the Cre recombinase needed only to remove *Frs2* from one allele. Results showed that the incidence of abnormality in these two lines was similar to the line with one allele of RNase10-Cre and two alleles of *loxP*-flanked *Frs2* ($Frs2^{cko/cko}$ *RNase10*-Cre^{tg}) (Table 1). Therefore, the variety of

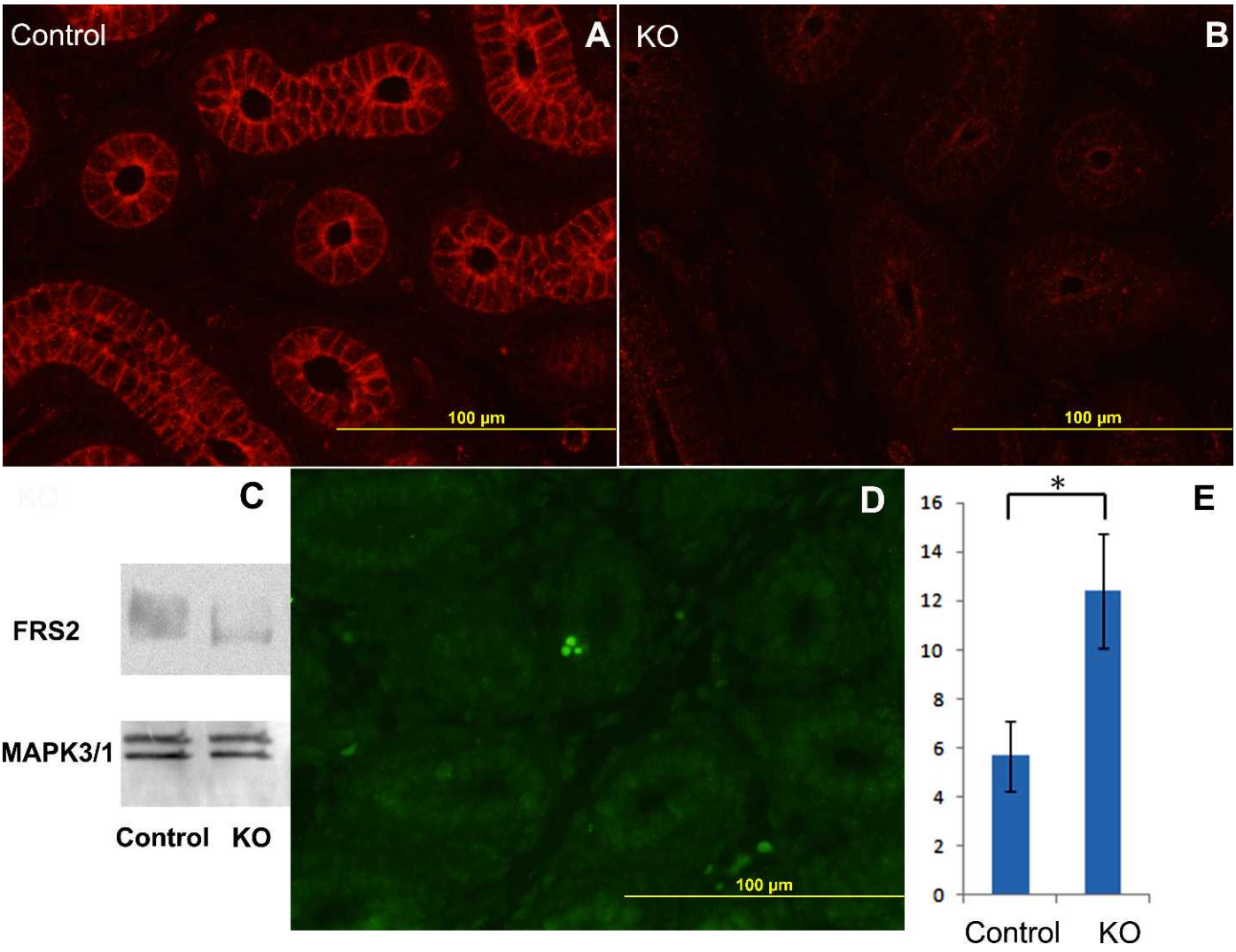

FIG 3. Increased apoptotic events in the epididymis after deletion of *Frs2* by Hoxb7-Cre during the undifferentiated period of postnatal development. Phospho-FRS2 immunolabeling in the caput largely decreased in the P10 knockout epididymis (**B**, $Frs2^{cko/-}$ *Hoxb7-Cre*^{tg}) compared to the control (**A**, $Frs2^{flox/-}$). Western blot analysis indicated that the FRS2 protein expression in P10 epididymal tissues (excluding the IS) decreased following deletion of *Frs2* by Hoxb7-Cre; immunoblotting of MAPK3/1 was used as loading control (**C**). A cluster of apoptotic cells was detected in a knockout epididymis by TUNEL labeling (**D**). Apoptotic incidence was increased in the knockout ($Frs2^{cko/-}$ *Hoxb7-Cre*^{tg}) compared to the controls ($Frs2^{flox/-}$ or $Frs2^{cko/+}$ *Hoxb7-Cre*^{tg}) (**E**). The epididymides from 10 pairs of knockout and litter mate controls from P4 to P14 were examined. The apoptotic index was calculated by the number of apoptotic cells in the epithelium per square millimeter of the epididymal area. Error bars indicate SEM. *Significant differences ($P < 0.05$). Bars = 100 μm (**A**, **B**, and **D**).

phenotypes was not caused by the recombination efficiency of RNase10-Cre.

The morphology of the abnormal epididymides was studied in detail (Fig. 7). Even in the abnormally shaped epididymides (Fig. 6, B and C), the epithelial cells in the IS (Fig. 7A) had undergone differentiation, as shown by higher epithelial height and higher phospho-MAPK3/1 level than in the caput (Fig. 7B). However, clusters of apoptotic cells (Fig. 7C) and disrupted tubules (Fig. 7D, arrow) were detected in the IS and caput of the abnormally shaped epididymides. Spermatozoa were observed exuding out of a disrupted tubule (Fig. 7E). The development of a granuloma was observed around exuded spermatozoa in a knockout epididymis (Fig. 7F).

Impact of Frs2 *Deletion Driven by RNase10-Cre on the Components of Signal Transduction Pathways in the Adult IS and Caput*

The adult knockout epididymides ($Frs2^{cko/-}$ *RNase10*-Cre^{tg}) with normal morphology were further analyzed to study the impact of *Frs2* deletion on signal transduction pathways in the proximal epididymis. First, as shown in Figure 8A (blue bars), after deletion of *Frs2* from the IS epithelial cells, *Frs2* mRNA levels of the entire IS declined significantly ($P < 0.01$) to approximately 29% of the control ($Frs2^{flox/-}$) level**.** However, the mRNA expression levels of *Etv4*, *Dusp6*, and *Ret* were not affected by *Frs2* deletion. Notably, the activity levels of phospho-MAPK3/1 and the mRNA expression levels of *Etv4*, *Dusp6*, and *Ret* were distinctly higher in the IS than in the caput, even with the deletion of *Frs2* (Fig. 8, A and B).

Partial deletion of *Frs2* from the caput epithelium did not cause a significant reduction of *Frs2* mRNA expression in the

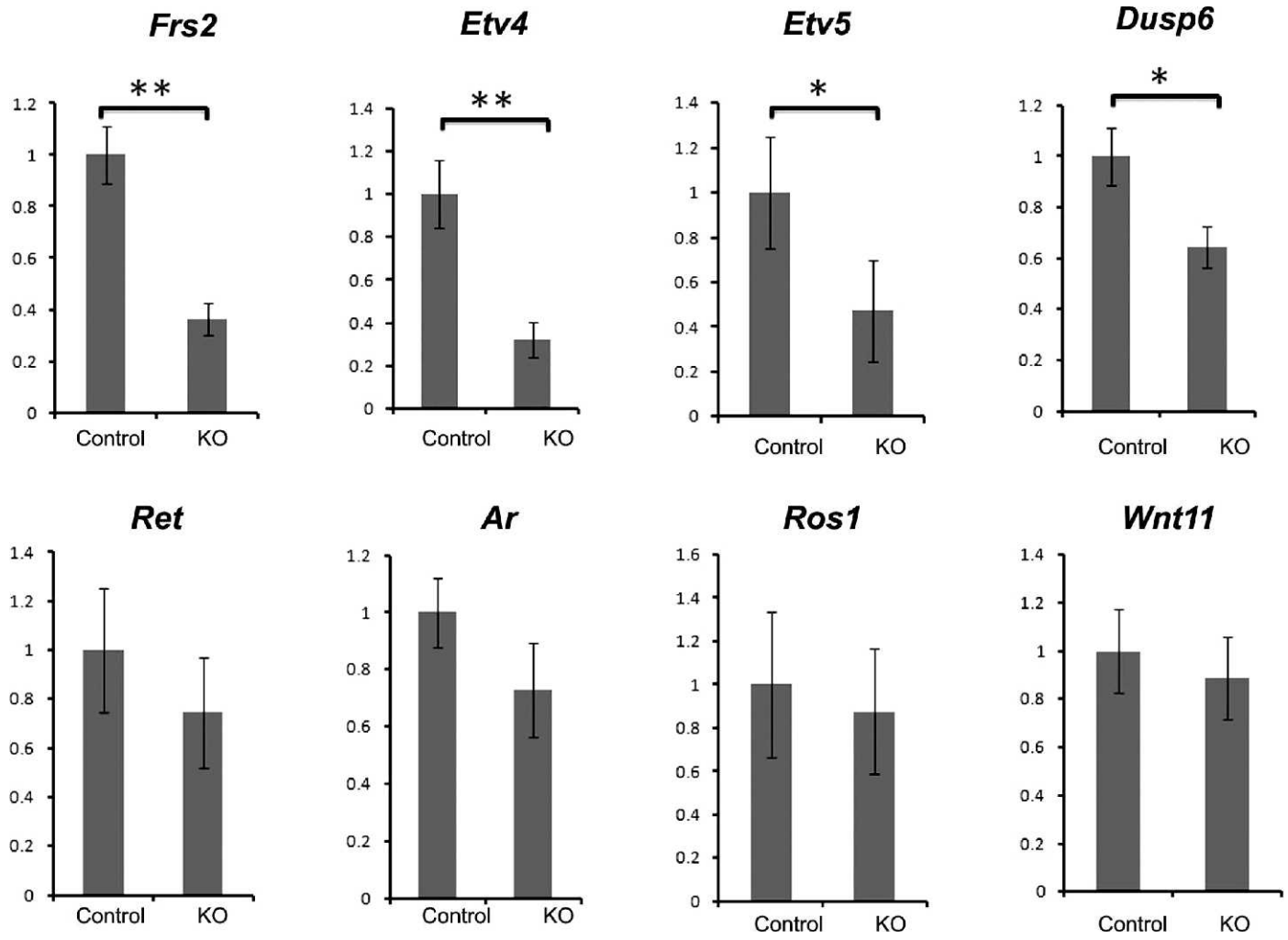

FIG 4. Impact of conditional deletion of *Frs2* by Hoxb7-Cre on the mRNA expression of key components of several signal transduction pathways. Total mRNA was isolated from P14 epididymides, excluding the IS. Messenger RNA levels of *Frs2*, *Dusp6*, *Etv4*, *Etv5*, *Ret*, *Ar*, *Ros1*, *and Wnt11* expression in the knockout ($Frs2^{cko/-}$ *Hoxb7-Cre*^{tg}) and control ($Frs2^{flox/-}$) samples were quantified. Deletion of *Frs2* from the epithelial cells resulted in a significant reduction of *Frs2* mRNA expression (upper panel). The mRNA levels of *Etv4*, *Etv5*, and *Dusp6* expression declined significantly after loss of *Frs2* (upper panel); levels of mRNA *Ret, Ar, Ros1, and Wnt11* expression, however, were not significantly altered by *Frs2* deletion (lower panel). Error bars indicate SEM. Asterisks indicate significant differences as follows: $*P < 0.05$; $**P < 0.01$. Four replicates were included in each group.

knockout group (Fig. 8A, red bars). The effect of *Frs2* partial deletion did not significantly reduce the mRNA expression of *Etv4*, *Dusp6*, and *Ret* in the caput.

DISCUSSION

Use of Cre Lines for Epididymis-Specific Gene Knockouts

Conditional knockout of genes from the epididymis has been hampered by the lack of epididymis-specific Cre lines. However, Hoxb7-Cre has been used to induce DNA recombination in epithelium of the Wolffian duct during the embryonic period. Also, a Hoxb7-Cre line has been used to remove a targeted gene from ureteric epithelium, which develops from the posterior part of the Wolffian duct [13]. Therefore, our study used a Hoxb7-Cre line [14] to conditionally knock out a gene in the epididymis, which develops from the anterior part of Wolffian duct. Three aspects were observed when we used a Hoxb7-Cre line for epididymal-specific gene knockout experiments: First, Hoxb7-Cre achieved efficient recombination in most of the epididymal epithelium, including the caput, corpus, and cauda, but a mosaic pattern was also observed in these regions (Fig. 2C). Second, the recombination efficiency of Hoxb7-Cre was much lower in the IS than in the caput (Fig. 2), even during the undifferentiated period when the IS and caput did not show any morphological differences. Third, Hoxb7-Cre is also expressed in ureteric epithelium; therefore, the targeted gene was deleted from ureteric epithelium in addition to epididymal epithelium. When we analyzed epididymal phenotypes of the targeted gene deletion induced by Hoxb7-Cre, it was necessary to rule out any secondary defects caused by gene deletion in the ureteric epithelium.

An RNase10-Cre line was recently established by Dr. Huhtaniemi's group and was used to successfully delete the *Ar* gene from the proximal epididymis [15]. In this study, we crossed the RNase10-Cre line with three *loxP* mouse lines. Our results further proved that the RNase10-Cre line was a useful tool for the conditional deletion of targeted genes from the IS epithelium from the period of differentiation onward: 1) when crossing with mT/mG Cre reporter mice, RNase10-Cre rapidly achieved almost complete recombination among most of the IS epithelial cells except for the narrow cells (Fig. 5A), which accounted only for approximately 3% of the IS epithelial cells [6]. Interestingly, RNase10-Cre was not functional in the

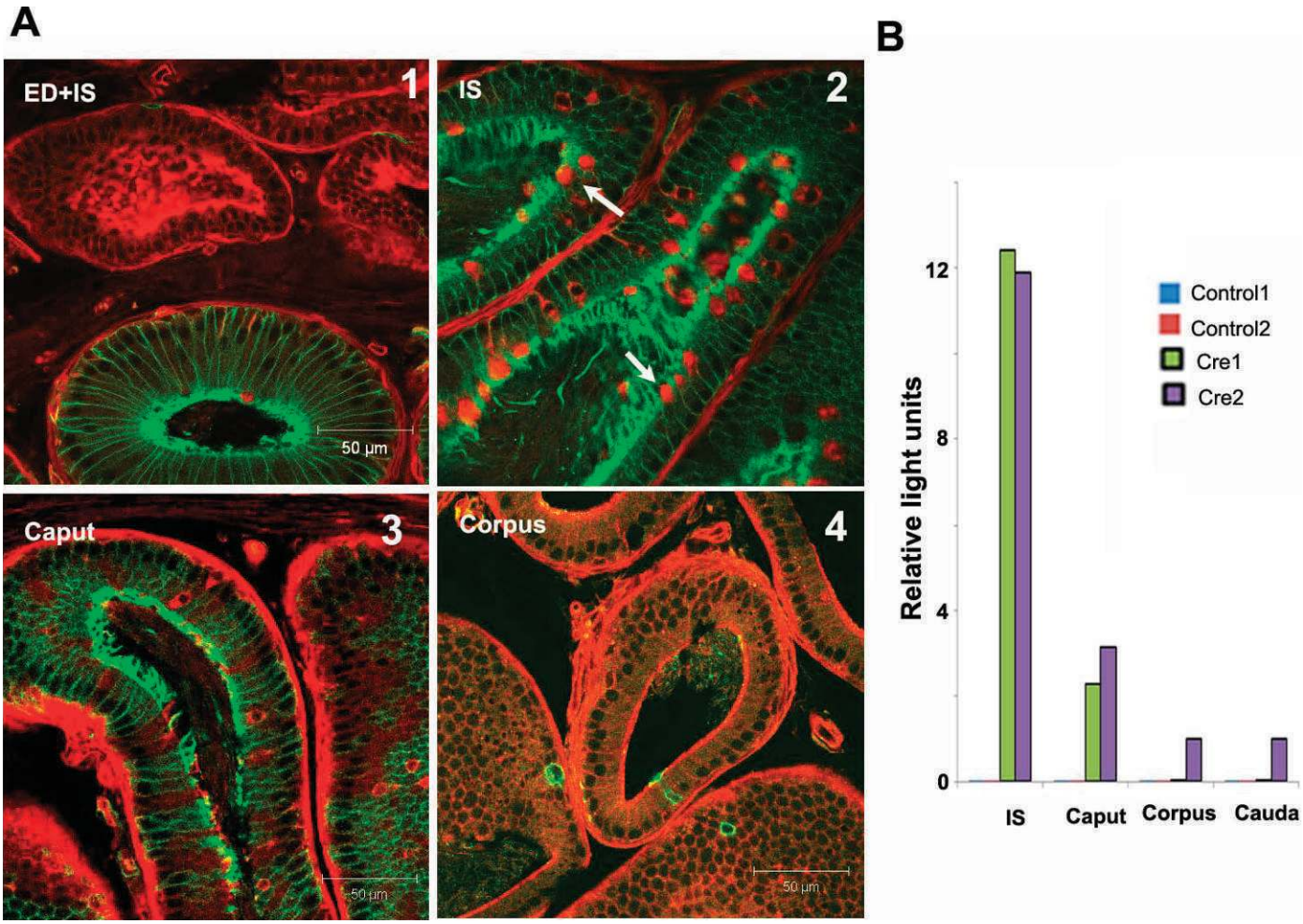

FIG 5. Recombination efficiency of RNase10-Cre in epididymal regions. **A**) Recombination efficiency of RNase10-Cre tested by breeding RNase10-Cre mice with mT/mG Cre reporter mice. The change of fluorescent color on the cell membrane from red to green indicated a recombination event induced by RNase10-Cre. RNase10-Cre recombination was rarely detected in the efferent ducts (**1,** upper tubule). Recombination occurred in most of the epithelial cells except for narrow cells (arrows) in the IS (**1** lower tubule, **2**). A mosaic recombination pattern was found in the proximal caput epithelium (**3**), and recombination events were rarely detected in the corpus (**4**). Bars = 50 μm. **B**) Recombination efficiency of RNase10-Cre tested by breeding RNase10-Cre mice with luciferase Cre reporter mice. Luciferase activities in the epididymides were measured in two luciferase Cre reporter mice expressing RNase10-Cre (Cre1, Cre2) and two control mice not expressing RNase10-Cre (Control 1, Control 2). The two RNase10-Cre nonexpressing controls had a very low background level of luciferase activity. Cre1 and Cre2 showed strong luciferase activity in the IS, ~80% less activity in the caput compared to the IS, and a lower level of activity in the corpus and cauda.

narrow cells, presumably because of cell type-specific activity of RNase10 promoter. 2) When crossing with luciferase Cre reporter mice, RNase10-Cre achieved a high recombination efficiency in the IS, and a weak recombination in the caput (Fig. 5B). 3) When crossing with *loxP*-flanked *Frs2* mice, RNase10-Cre reduced *Frs2* mRNA level of the entire IS to approximately 29% of the control level. Considering RNase10-Cre was not functional in IS interstitial tissues that may have contributed to some of the remaining 29% *Frs2* mRNA expression, RNase10-Cre was highly efficient in IS epithelial cells. Furthermore, increasing allele numbers of RNase10-Cre or decreasing allele numbers of loxP-flanked *Frs2* did not further increase the recombination efficiency, therefore indicating high efficiency of a single allele of RNase10-Cre.

TABLE 1. Incidence of abnormality after deletion of *Frs2* from the epithelial cells of the proximal epididymis from P17 onward.

	Abnormality in controls (n)			Abnormality in knockout mice (n)		
Genotype	$Frs2^{flox/flox}$*	$Frs2^{cko/+}$ *Rnase10*-Cre^{tg}*	$Frs2^{flox/-}$†	$Frs2^{cko/cko}$ *Rnase10*-Cre^{tg}*	$Frs2^{cko/cko}$ *Rnase10*-$Cre^{tg/tg}$*	$Frs2^{cko/-}$ *Rnase10*-Cre^{tg}†
Abnormal shape	0%	0%	0%	10.7%	13.6%	9.4%
Blockage	5.1%	3.0%	4.9%	10.7%	9.1%	12.5%
Total abnormality	5.1% (118)	3.0% (40)	4.9% (41)	21.4% (112)	22.7% (22)	21.9% (32)

* By crossing $Frs2^{flox/flox}$ mice with *RNase10*-Cre^{tg} mice, we generated the conditional knockout $Frs2^{cko/cko}$ *RNase10*-Cre^{tg}, $Frs2^{cko/cko}$ *RNase10*-$Cre^{tg/tg}$ and the littermate controls $Frs2^{cko/+}$ *RNase10*-Cre^{tg}, $Frs2^{flox/flox}$.

† By crossing $Frs2^{flox/flox}$ mice with *E11a*-Cre^{tg} mice, we first generated *Frs2* heterozygous $Frs2^{+/-}$, then by crossing $Frs2^{+/-}$ mice with $Frs2^{cko/+}$ *RNase10*-Cre^{tg} mice, we generated $Frs2^{cko/-}$ *RNase10*-Cre^{tg} knockout mice and $Frs2^{flox/-}$ control mice.

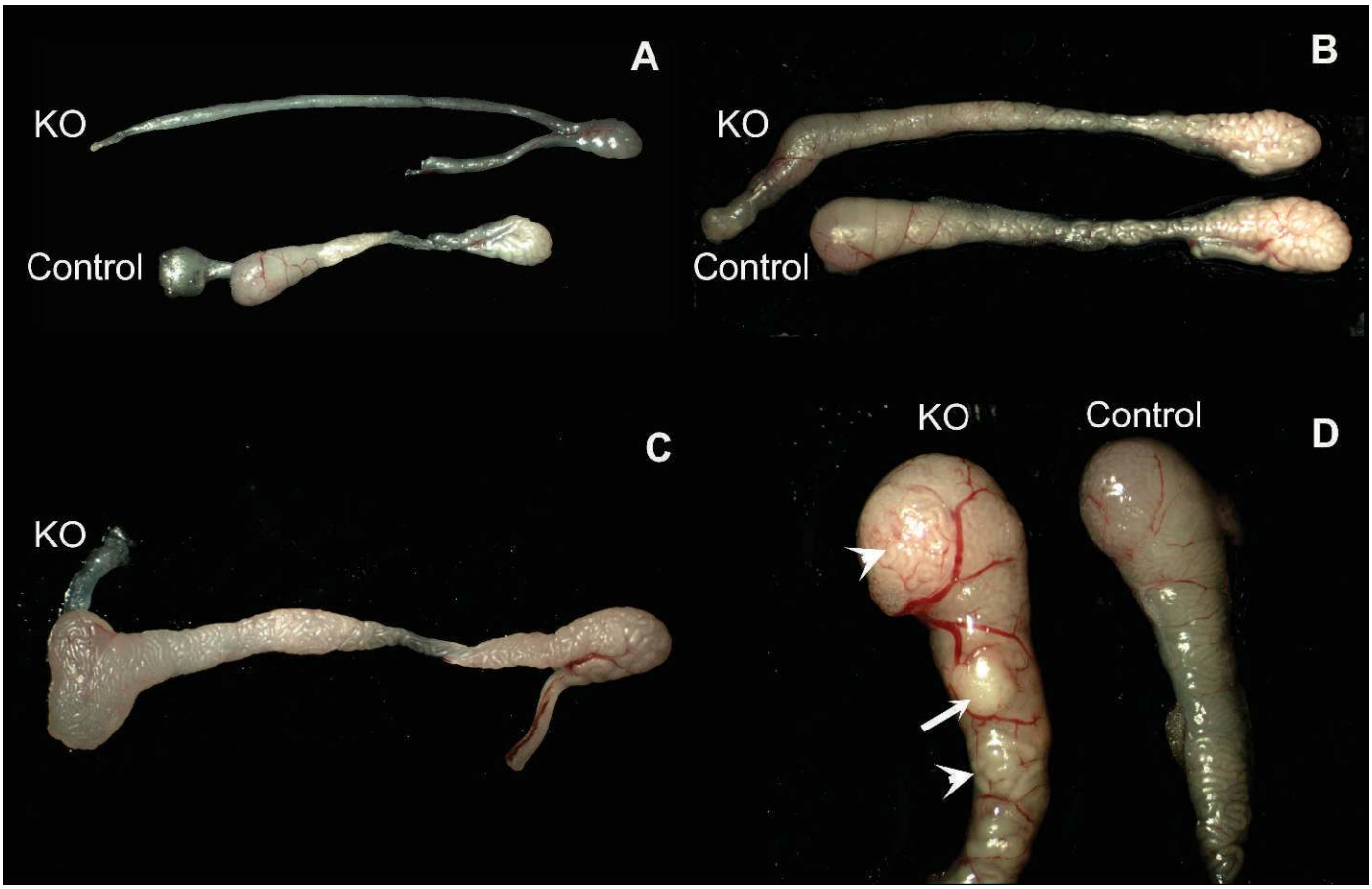

FIG 6. Phenotypes after loss of *Frs2* from the proximal epididymal epithelium. Deletion of *Frs2* from epithelial cells of the proximal epididymis resulted in abnormal epididymides in a subgroup of mice with a range of variety, including smaller proximal epididymides (**A**), abnormally shaped proximal epididymides (**B** and **C**), obstruction of sperm flow (arrowheads), and development of a granuloma (arrow) at the proximal epididymal region (**D**). **D**) The control normal epididymal tubule in the IS and caput looks translucent under a dissection scope. In the knockout epididymis, the blocked tubule with sperm flow obstruction looks opaque and its tubule diameter increased (arrowhead). The granuloma site has no clear tubule structure; it looks like an opaque mass surrounded by the blocked tubule and is protruded (arrow).

Differential Expression and Localization of FRS2 During Postnatal Epididymal Development

FRS2 protein expression, phosphorylation, and localization in the epididymis showed dynamic changes during the transition from the undifferentiated period to the period of differentiation (between P14 and P21). FRS2 had high expression and phosphorylation levels during the undifferentiated period. The activated (phosphorylated) form of FRS2 was localized mainly to both the basolateral and the apical membranes of epithelial cells among each epididymal region. By contrast, FRS2 expression and phosphorylation levels declined from the period of differentiation onward; the activated form of FRS2 was localized mainly to the apical membrane of the IS epithelial cells (Fig. 1).

It was shown previously that activated RTKs, which were bound with their ligands, recruited FRS2 to cell the membrane and phosphorylated FRS2 at tyrosine sites. Activated FRS2 then activated multiple signal transduction pathways [10]. Dynamic changes of FRS2 expression, phosphorylation, and localization during the transition from the undifferentiated period to the period of differentiation implicated differential functions of FRS2 in these two periods.

Our Western blot data (Fig. 1A) correlated with our IF data (Fig. 1B). Western blot analysis detected a series of FRS2 protein bands indicating polymorphism of FRS2 molecular mass because of posttranslation modification. From P21 onward, the FRS2 bands shifted toward lower molecular weights in the caput, presumably caused by dephosphorylation. Consistently, our IF experiment detected a decline in FRS2 phosphorylation level in the caput from P21 onward.

Regulation of the Basal Activity Level of the Components of the ERK Pathway

The undifferentiated epididymal epithelium had a basal activity level of the ERK pathway components, and this basal level remained in most of the epididymal epithelium, except for the IS epithelium, from the period of differentiation onward [8]. The regulation of this basal level of activity is unclear. Previous studies have surveyed the expression of growth factors in the epididymis and indicated the regional specific expression patterns for several growth factors [18, 19]. A recent knockout study demonstrated that FGF8, which is expressed in the male reproductive tract, was essential for the formation of the ductal system in the epididymis, vas deferens, and efferent ducts [20]. Overexpression of FGF8b caused progressive stromal and epithelial changes in the epididymis in transgenic mice [21]. These findings suggest that growth factor signaling is important for epididymal development. However, a connection between growth factor signaling and the basal activity level of

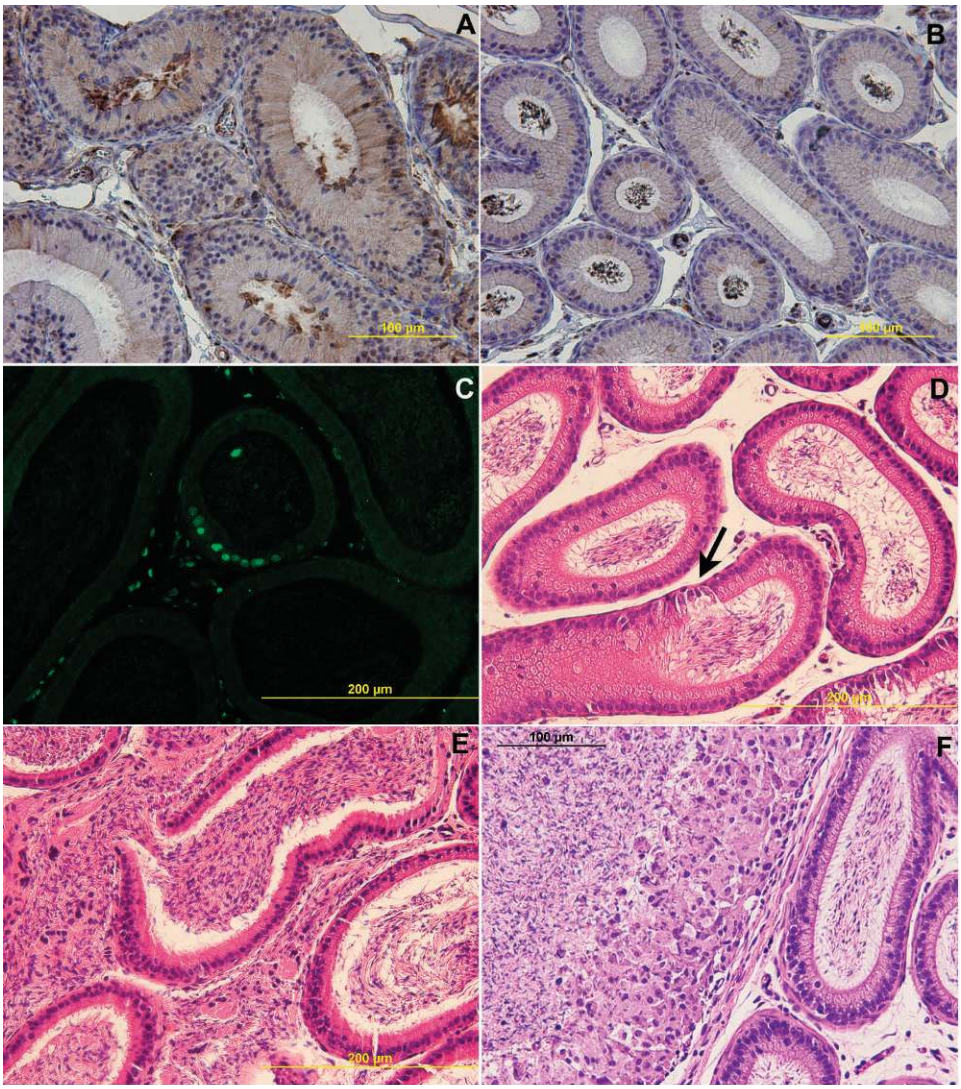

FIG 7. Morphology of abnormal epididymides with a conditional deletion of *Frs2* from the proximal epididymal epithelium. Even an abnormally shaped epididymis had differentiated epithelial cells in the IS (**A**), marked by greater height and higher phospho-MAPK3/1 levels than those of the caput (**B**). A cluster of apoptotic cells in the IS (**C**) was detected by TUNEL labeling, and a broken tubule in the proximal caput (**D**, arrow) was observed in the knockout epididymides. Spermatozoa were observed escaping from a broken tubule in the proximal caput area (**E**), and the development of a granuloma in the proximal caput area (**F**) was observed in the knockout epididymides. Bars = 100 µm (**A**, **B**, and **F**) or 200 µm (**C**–**E**).

the components of the ERK pathway in the epididymal epithelium needs to be further investigated.

During the undifferentiated period, FRS2 had a strong expression level, and activated FRS2 was located at both the basolateral and the apical membranes of epithelial cells in the epididymis. Therefore, in our first mouse model, *Frs2* was deleted in the epithelial cells of most epididymal regions from the embryonic period onward. This conditional knockout model was used to test the role of FRS2 in the regulation of the basal activity level of the components of the ERK pathway.

Deletion of *Frs2* indeed attenuated the basal activity level of the components of the ERK pathway, which were detected in $Frs2^{cko/-}$ *Hoxb7-Cre*^{tg} knockout mice. The attenuated basal activity level of the components of the ERK pathway resulted in an increase in apoptosis along the epididymal duct during the undifferentiated period, the same time period when FRS2 had the highest protein expression level in wild-type epididymides. It is possible that FRS2 was minimally involved in the regulation of the basal activity level of the components of the ERK pathway at later periods because FRS2 expression and activity levels were lower from the period of differentiation onward (Fig. 1). Deletion of *Frs2* from epithelial cells of most epididymal regions except for the IS had no significant effect on cell survival from the period of differentiation onward.

Deletion of *Frs2* by Hoxb7-Cre removed *Frs2* not only from the epididymal epithelium but also from the ureteric epithelium. A previous study indicated that ablation of Frs2 from the ureteric epithelium resulted only in a mild phenotype, and kidney function was not seriously impaired [13]. Therefore, the phenotype we observed here is unlikely caused by any secondary defects from the kidney defect.

In $Frs2^{cko/-}$ *Hoxb7-Cre*^{tg} epididymides, apoptotic cells were often found as a cluster during the undifferentiated period. However, the clustered apoptotic cells did not accumulate or remain in the epithelium. Instead, apoptotic cells were often observed inside the lumen, implicating the removal of apoptotic cells through the lumen. It would presumably be advantageous to remove apoptotic cells from the epithelium, because these apoptotic cells might cause disruption and block spermatozoa along the epididymal duct during the expansion

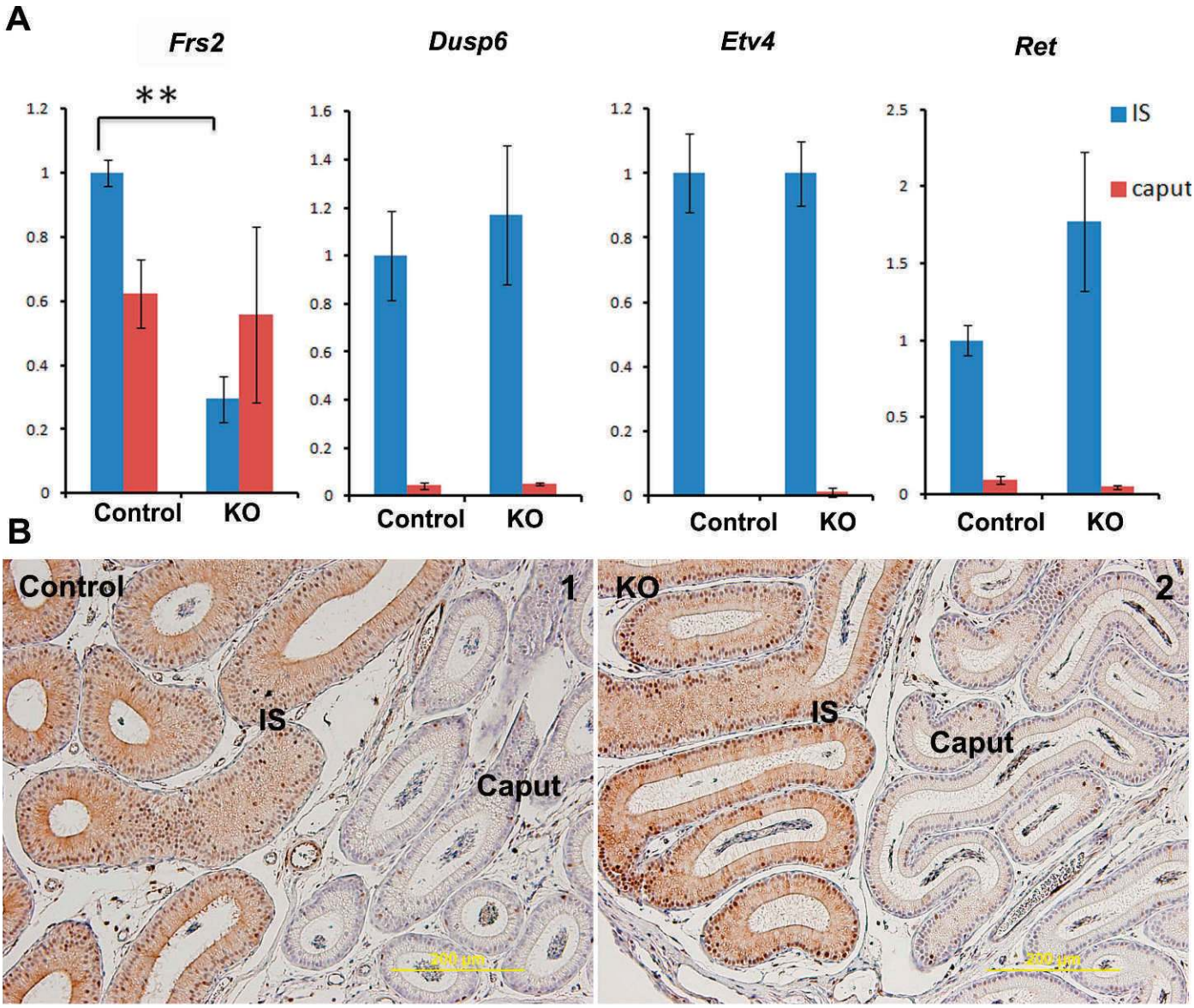

FIG 8. Impact of deletion of *Frs2* from the proximal epididymal epithelium on mRNA expression of the components of signal transduction pathways. **A**) Quantification of levels of *Frs2*, *Dusp6*, *Etv4*, and *Ret* mRNA expression in the IS (blue bars) and caput (red bars) from the normal morphological knockout ($Frs2^{cko/-}$ *RNase10*-Cre^{tg}) and control ($Frs2^{flox/-}$) samples. The *Frs2* mRNA level in the IS of this knockout group was reduced to ~29% of the control level after loss of *Frs2* from the IS epithelium**,** but mRNA expression levels of *Etv4*, *Dusp6*, and *Ret* in the IS of this knockout group were not significantly affected by *Frs2* deletion. Partial deletion of *Frs2* from the caput epithelium of this knockout group did not cause a significant reduction of *Frs2* mRNA expression in the caput and did not significantly affect mRNA expression of *Dusp6*, *Etv4*, and *Ret*. **B**) Representative images of IHC labeling of phospho-MAPK3/1 in the IS and caput of the control ($Frs2^{flox/-}$) and the normal morphological knockout ($Frs2^{cko/-}$ *RNase10*-Cre^{tg}) samples. Loss of *Frs2* did not impair the high activity levels of MAPK3/1 in the IS epithelium of this knockout group. Notably, the activity levels of MAPK3/1 and mRNA expression levels of *Etv4*, *Dusp6*, and *Ret* were distinctly higher in the IS than in the caput in both the knockout and the control groups. Error bars indicate SEM. **Significant differences ($P < 0.01$). Bars = 200 μm.

period. Removal of a large number of apoptotic cells from the epididymal epithelium through the lumen following EDL has also been observed in other studies [19].

Regulation of the High Activity Level of the Components of the ERK Pathway in the IS Epithelium

From the period of differentiation onward, the activity level of the components of the ERK pathway was distinctly higher in the IS epithelium than in other regions [8]. As mentioned above, lumicrine factors were responsible for stimulating and sustaining this high activity level. Lumicrine regulation [22] has been shown to be essential for IS cell proliferation, differentiation, and survival [7, 8]. Although several growth factors were detected in luminal fluid and several RTKs were located within epithelial cells of the IS [23, 24], the direct connection between lumicrine growth factor signaling and high activity level of the components of the ERK pathway in the IS needs to be further established.

From the period of differentiation onward, activated FRS2 was observed mainly at the apical membrane of the IS epithelial cells. It is reasonable to hypothesize that apically expressed FRS2 regulated the high activity level of the components of the ERK pathway in the IS epithelium. Therefore, in our second mouse model, *Frs2* was removed

from the epithelium of the proximal epididymis from P17 onward to test this hypothesis.

Efficient deletion of *Frs2* from the IS epithelium did not affect either the high levels of MAPK3/1 activities or the high levels of mRNA expression of *Etv4* and *Dusp6* in most of the *Frs2*$^{cko/-}$ *RNase10*-Cre^{tg} knockout IS (Fig. 8). Even among abnormally shaped knockout epididymides, high MAPK3/1 phosphorylation levels were detected in IS epithelium (Fig. 7). Apparently, FRS2 was not the sole upstream regulator responsible for activation of the components of the ERK pathway in the IS.

It is possible that FRS2 was just one of the adaptor proteins responding to lumicrine growth factors and transmitting the signals from RTKs to the intracellular signal transduction pathways. Furthermore, FRS2 function could be compensated by other RTK adapter proteins such as FRS3 (also named FRS2beta), v-crk sarcoma virus CT10 oncogene homolog (CRK), phospholipase C, gamma (PLCG), and Src homology 2 domain containing protein (SHC) [13, 25–27].

Besides growth factors, a high concentration of androgens is also found in luminal fluid [28]. Therefore, it is also possible that luminal growth factors maintained the permissive activity level of the ERK pathway components, while luminal androgens stimulated the high activity level of the components of the ERK pathway in the IS. Androgen signaling may bypass FRS2 to regulate MAPK3/1 and downstream targets through the androgen receptor (AR) nongenomic action [29].

The mice with targeted deletion of *Frs2* induced by RNase10-Cre had a mixed background of 129 and C57B6 strains. It is possible that the abnormal phenotype shown in the subgroup caused by compensation from other genes did not fully compensate the loss of *Frs2* in a certain genetic background.

In summary, our first knockout model provided evidence that FRS2 regulated the basal activity level of the components of the ERK pathway during the undifferentiated period of postnatal epididymal development. The reduced basal activity level caused by *Frs2* deletion correlated with increased apoptotic events. Our second knockout model provided evidence that FRS2 was not the sole upstream regulator responsible for the activation of the components of the ERK pathway in IS epithelium from the period of differentiation onward. However, a subgroup of mice in our second knockout model showed abnormal epididymides caused by apoptosis. Taken together, these two conditional *Frs2* knockout models provided useful tools for understanding the molecular mechanism by which intercellular signaling regulates epididymal development.

ACKNOWLEDGMENT

We thank Dr. Fen Wang (University of Texas A&M) for providing mice carrying the *loxP*-flanked *Frs2* allele, Dr. Ilpo Huhtaniemi (Imperial College London, UK) for providing Tg(RNase10-Cre) mice line, and Dr. Jing Yu (University of Virginia) for providing Tg(Hoxb7-Cre) mice line.

REFERENCES

1. Hinton BT, Galdamez MM, Sutherland A, Bomgardner D, Xu B, Abdel-Fattah R, Yang L. How do you get six meters of epididymis inside a human scrotum? J Androl 2011; 32:558–564.
2. Jiang FX, Temple-Smith P, Wreford NG. Postnatal differentiation and development of the rat epididymis: a stereological study. Anat Rec 1994; 238:191–198.
3. Robaire B, Hinton BT, Orgebin-Crist MC. The epididymis In: Neill JD (ed.), Knobil and Neill's Physiology of Reproduction, 3rd ed. New York: Elsevier; 2006: 1071–1148.
4. Welsh M, Saunders PT, Sharpe RM. The critical time window for androgen-dependent development of the Wolffian duct in the rat. Endocrinology 2007; 148:3185–3195.
5. Rodriguez CM, Kirby J, Hinton BT. The development of the epididymis In: Robaire B, Hinton BT (eds.), The Epididymis From Molecules To Clinical Practice. New York: Kluwer Academic/Plenum Publishers; 2002: 251–267.
6. Robaire B, Hermo L. Efferent duct, epididymis, and vas deferens: structure, functions, and their regulation In: Knobil E, Neill JD (eds.), The Physiology of Reproduction, vol. 1. New York: Raven Press; 1988: 999–1080.
7. Xu B, Abdel-Fattah R, Yang L, Crenshaw SA, Black MB, Hinton BT. Testicular lumicrine factors regulate ERK, STAT, and NFKB pathways in the initial segment of the rat epididymis to prevent apoptosis. Biol Reprod 2011; 84:1282–1291.
8. Xu B, Yang L, Lye RJ, Hinton BT. p-MAPK1/3 and DUSP6 regulate epididymal cell proliferation and survival in a region-specific manner in mice.Biol Reprod 2010; 83:807–817.
9. Jegou B, Le Gac F, de Kretser DM. Seminiferous tubule fluid and interstitial fluid production. I. Effects of age and hormonal regulation in immature rats.Biol Reprod 1982; 27:590–595.
10. Gotoh N. Regulation of growth factor signaling by FRS2 family docking/scaffold adaptor proteins. Cancer Sci 2008; 99:1319–1325.
11. Zhang Y, Zhang J, Lin Y, Lan Y, Lin C, Xuan JW, Shen MM, McKeehan WL, Greenberg NM, Wang F. Role of epithelial cell fibroblast growth factor receptor substrate 2alpha in prostate development, regeneration and tumorigenesis. Development 2008; 135:775–784.
12. Zhang J, Lin Y, Zhang Y, Lan Y, Lin C, Moon AM, Schwartz RJ, Martin JF, Wang F. Frs2alpha-deficiency in cardiac progenitors disrupts a subset of FGF signals required for outflow tract morphogenesis. Development 2008; 135:3611–3622.
13. Sims-Lucas S, Cullen-McEwen L, Eswarakumar VP, Hains D, Kish K, Becknell B, Zhang J, Bertram JF, Wang F, Bates CM. Deletion of Frs2alpha from the ureteric epithelium causes renal hypoplasia. Am J Physiol Renal Physiol 2009; 297:F1208–1219.
14. Yu J, Carroll TJ, McMahon AP. Sonic hedgehog regulates proliferation and differentiation of mesenchymal cells in the mouse metanephric kidney. Development 2002; 129:5301–5312.
15. Krutskikh A, De Gendt K, Sharp V, Verhoeven G, Poutanen M, Huhtaniemi I. Targeted inactivation of the androgen receptor gene in murine proximal epididymis causes epithelial hypotrophy and obstructive azoospermia. Endocrinology 2011; 152:689–696.
16. Krutskikh A, Poliandri A, Cabrera-Sharp V, Dacheux JL, Poutanen M. Epididymal protein RNase10 is required for post-testicular sperm maturation and male fertility. FASEB J 2012; 26:4198–209.
17. Zhang Y, McKeehan K, Lin Y, Zhang J, Wang F. Fibroblast growth factor receptor 1 (FGFR1) tyrosine phosphorylation regulates binding of FGFR substrate 2alpha (FRS2alpha) but not FRS2 to the receptor. Mol Endocrinol 2008; 22:167–175.
18. Tomsig JL, Turner TT. Growth factors and the epididymis. J Androl 2006; 27:348–357.
19. Turner TT, Johnston DS, Finger JN, Jelinsky SA. Differential gene expression among the proximal segments of the rat epididymis is lost after efferent duct ligation. Biol Reprod 2007; 77:165–171.
20. Kitagaki J, Ueda Y, Chi X, Sharma N, Elder CM, Truffer E, Costantini F, Lewandoski M, Perantoni AO. FGF8 is essential for formation of the ductal system in the male reproductive tract. Development 2011; 138: 5369–5378.
21. Elo T, Sipila P, Valve E, Kujala P, Toppari J, Poutanen M, Harkonen P. Fibroblast growth factor 8b causes progressive stromal and epithelial changes in the epididymis and degeneration of the seminiferous epithelium in the testis of transgenic mice. Biol Reprod 2012; 86:157.
22. Hinton BT, Lan ZJ, Lye RJ, Labus JC. Regulation of epididymal function by testicular factors: The lumicrine hypothesis In: Goldberg E (ed.), The Testis. New York: Springer-Verlag; 2000: 163–173.
23. Lan ZJ, Labus JC, Hinton BT. Regulation of gamma-glutamyl transpeptidase catalytic activity and protein level in the initial segment of the rat epididymis by testicular factors: role of basic fibroblast growth factor. Biol Reprod 1998; 58:197–206.
24. Kirby JL, Yang L, Labus JC, Hinton BT. Characterization of fibroblast growth factor receptors expressed in principal cells in the initial segment of the rat epididymis. Biol Reprod 2003; 68:2314–2321.
25. Gotoh N, Laks S, Nakashima M, Lax I, Schlessinger J. FRS2 family docking proteins with overlapping roles in activation of MAP kinase have distinct spatial-temporal patterns of expression of their transcripts. FEBS Lett 2004; 564:14–18.
26. Sims-Lucas S, Cusack B, Eswarakumar VP, Zhang J, Wang F, Bates CM.

Independent roles of Fgfr2 and Frs2alpha in ureteric epithelium. Development 2011; 138:1275–1280.
27. Powers CJ, McLeskey SW, Wellstein A. Fibroblast growth factors, their receptors and signaling. Endocr Relat Cancer 2000; 7:165–197.
28. Turner TT, Jones CE, Howards SS, Ewing LL, Zegeye B, Gunsalus GL. On the androgen microenvironment of maturing spermatozoa. Endocrinology 1984; 115:1925–1932.
29. Hamzeh M, Robaire B. Androgens activate mitogen-activated protein kinase via epidermal growth factor receptor/insulin-like growth factor 1 receptor in the mouse PC-1 cell line. J Endocrinol 2011; 209:55–64.